FOI-R--0723--SE
November 2002
ISSN 1650-1942
Scientific report

Peter Skoglund

Constitutive modelling and mechanical properties of a tungsten heavy metal alloy

Weapons and Protection
SE-147 25 Tumba

SWEDISH DEFENCE RESEARCH AGENCY
Weapons and Protection
SE-147 25 Tumba

FOI-R--0723--SE
November 2002
ISSN 1650-1942
Scientific report

Peter Skoglund

Constitutive modelling and mechanical properties of a tungsten heavy metal alloy

Issuing organization	Report number, ISRN	Report type
FOI – Swedish Defence Research Agency Weapons and Protection SE-147 25 Tumba	FOI-R--0723--SE	Scientific report
	Research area code 5. Combat	
	Month year November 2002	**Project no.** E2008
	Customers code 5. Commissioned Research	
	Sub area code 51 Weapons and Protection	

Author/s (editor/s)	Project manager
Peter Skoglund	Lars Holmberg
	Approved by
	Sponsoring agency
	Scientifically and technically responsible

Report title

Constitutive modelling and mechanical properties of a tungsten heavy metal alloy

Abstract (not more than 200 words)

The mechanical behaviour of a tungsten heavy metal alloy (WHA) with potential use as a kinetic energy penetrator is investigated. From quasi-static experiments the deduced flow stress curves are discussed and the ultimate tensile stress is compared to the suppliers data. Dynamic mechanical properties related to tensile loading are measured at strain rates up to 400 s^{-1} and at temperatures from 20 °C to about 500 °C. From the experimental data parameters for the constitutive equations developed by Johnson and Cook (J&C) as well as Zerilli and Armstrong (Z&A) are determined. The specific heat capacity is measured at temperatures from 20-200 °C and is used for calculations of the deformation induced temperature increase. From the extracted models isothermal and adiabatic flow stress curves are calculated and compared to experiments and available literature data.

The quasi-static experiments show a linear behaviour up to about 1300 MPa followed by a rather weak strain hardening, and fracture occurs at a nominal strain of the order of 5-10 %. The ultimate tensile stress is 1340 ± 30 MPa which is close to the value of 1350 MPa given by the manufacturer. At high strain rates or high temperatures the J&C model deviates about 5-10 % from experimental results, while the Z&A model shows a better agreement with the collected data. It should be emphasised that the Z&A model used in this work is developed for materials with body centred crystals whereas the WHA is a composite with both face centred- and body centred crystals.

Keywords

Heavy metal alloy, WHA, tungsten, constitutive model, mechanical properties

Further bibliographic information	Language English
ISSN 1650-1942	**Pages** 20 p.
	Price acc. to pricelist

Utgivare Totalförsvarets Forskningsinstitut - FOI Vapen och skydd 147 25 Tumba	**Rapportnummer, ISRN** FOI-R--0723--SE	**Klassificering** Vetenskaplig rapport
	Forskningsområde 5. Bekämpning	
	Månad, år November 2002	**Projektnummer** E2008
	Verksamhetsgren 5. Uppdragsfinansierad verksamhet	
	Delområde 51 VVS med styrda vapen	
Författare/redaktör Peter Skoglund	**Projektledare** Lars Holmberg	
	Godkänd av	
	Uppdragsgivare/kundbeteckning	
	Tekniskt och/eller vetenskapligt ansvarig	

Rapportens titel (i översättning)

Konstitutiv modellering och mekaniska egenskaper för en wolframlegering

Sammanfattning (högst 200 ord)

De mekaniska egenskaperna för en tungmetallegering av wolfram (WHA) med potential som pilprojektilmaterial har undersökts. Flytspänningskurvor bestämda under kvasistatiska förhållanden diskuteras och brottspänningen bestäms och jämförs med leverantörsdata. De dynamisk-mekaniska egenskaperna relaterade till dragbelastning med töjningshastigheter upp till 400 s^{-1} och vid temperaturer mellan 20 °C och 500 °C undersöks och resultaten används för att bestämma materialparametrar till de konstitutiva ekvationer som utvecklats av Johnson och Cook (J&C) samt Zerilli och Armstrong (Z&A). Den specifika värmekapaciteten i temperaturområdet 20-200 °C har uppmätts och resultaten används för att bestämma den deformationsberoende temperaturökningen. Från modellerna beräknas de isoterma och adiabatiska flytspänningskurvorna och dessa jämförs med experiment och tillgängliga litteraturdata.

Av de kvasistatiska mätningarna framgår att materialet uppvisar ett linjärt elastiskt beteende upp till cirka 1300 MPa följt av ett svagt plastiskt deformationshårdnande till brott vid en nominell töjning av storleksordningen 5-10 %. Brottspänningen är 1340 $\pm$ 30 MPa, vilket är nära leverantörens värde på 1350 MPa. Vid höga töjningshastigheter eller höga temperaturer avviker J&C-modellen med 5-10 % från experimentella data, medan Z&A ekvationen uppvisar bättre överensstämmelse med försöken. Det bör poängteras att den använda Z&A relationen är framtagen för material med rymdcentrerad kristallstruktur medan WHA är en komposit med både rymd- och ytcentrerade kristaller.

Nyckelord

Tungmetall, WHA, konstitutiv modell, mekaniska egenskaper

Övriga bibliografiska uppgifter	**Språk** Engelska
ISSN 1650-1942	**Antal sidor:** 20 s.
Distribution enligt missiv	**Pris: Enligt prislista**

CONTENTS

INTRODUCTION

The behaviour of solids during fast deformation, such as ballistic impact, is a complex function of the properties of the interacting materials. Both the mechanical and thermal properties must be considered. The relative influence of these properties on the outcome of an impact event also depends on impact velocity, geometry and size of the objects. Density and impact velocity are important since they determine the magnitude of the inertia forces and the kinetic energies which drive the event. For ballistic impact at very high velocities, i.e. several km/s or higher, the deformation is dominated by inertia forces, while mechanical and thermal properties get increasingly more important at lower impact velocities. Thus, the intermediate velocity regime where most ballistic impact phenomena occur is the most difficult to analyse since the mechanical and thermal behaviour of the materials significantly influence the resulting deformations. However, it is generally very difficult to determine these properties at the complex loading conditions that occur during impact with multiaxial stresses, high hydrostatic pressures and high deformation rates. Magness [1] gives a thorough description of the problems associated with ballistic impact of high density projectiles.

The hydrocodes usually employed to model penetration phenomena require, among other input data, a constitutive equation to describe the material response to distortion. In this work a heavy metal alloy based on tungsten (WHA) with potential use as a kinetic energy (KE) penetrator has been mechanically characterised at tensile strain rates ranging from 10^{-4} to 400 s^{-1} and at temperatures between 20 and 500 °C. The experimental data are used to assess material parameters for the constitutive equation developed by Zerilli and Armstrong [2] as well as for the relation suggested by Johnson and Cook [3]. The flow stresses calculated using the two models are compared and discussed together with available literature data. At high deformation rates, which prevail in penetration events, the process is mainly adiabatic and the temperature increase will affect the calculated flow stress. Thus, the adiabatic flow stress curves are calculated incorporating a temperature dependent heat capacity. Finally, from quasi-static experiments the ultimate tensile stress and its standard deviation is determined and discussed.

EXPERIMENTAL

The heavy metal alloy investigated was supplied by Kennametal Hertel, Germany, and consists of tungsten grains embedded in a matrix of nickel, iron, cobolt and dissolved tungsten. In table I below some important chemical and physical data provided by the supplier can be seen.

Table I. Tungsten heavy metal alloy, suppliers data. The matrix consists of Ni, Fe, Co and dissolved W.

WHA properties (Grade Y925)	
Tungsten weight %	92.5
Density	17.70 g/cm^3
Ultimate stress	1350 MPa
Yield stress $R_{P0.2}$	1300 MPa
Elongation (A_5)	10 %

Equipment and methods

For the quasi-static measurements of the flow stress curves, 12 test samples were manufactured according to figure 1 below. All of the quasi-static measurements are carried out with a servohydraulic mechanical testing system from MTS Systems. The force is measured with a 10 kN load cell and the displacement with a position sensor (linear variable differential transformer) supplied by MTS Systems. The data are collected at a nominal tensile strain rate of 10^{-4} s^{-1}.

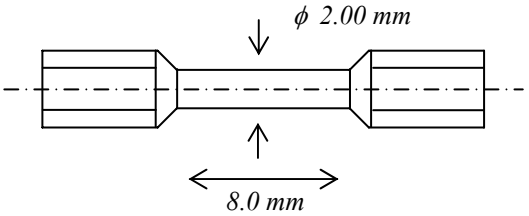

Figure 1. Geometry of the samples used for mechanical testing. The gauge length is 8.0 mm with a diameter of 2.00 mm. The specimen ends have M5 threads.

An additional series of experiments at nominal tensile strain rates 10^{-2}, 1, 10 and 400 s^{-1}, all at room temperature, as well as measurements at a constant strain rate of 1 s^{-1} but with temperatures from 20-500 °C were carried out aiming at obtaining data for a constitutive description of the WHA. The mechanical testing at strain rates up to 10 s^{-1} is carried out with the MTS equipment, while the results at the higher strain rates are obtained from experiments with a single bar Hopkinson device described by Svensson [4]. The data collected at enhanced sample temperatures are obtained using the servohydraulic testing equipment together with an induction heater. The temperature is measured with thermocouples and/or an IR-sensor on samples with a carbon black surface to give an emissivity of 0.85. The difference between the temperatures measured with the two methods was less than 10 °C. The specimen dimensions can be seen in figure 1.

The experimental raw data measured with the commercial MTS-system as described above were corrected for play and compliance of the structure connecting the sample with the displacement sensor. Further, since the constitutive equations require knowledge of the plastic deformation, the elastic part of the specimen deformation is subtracted and the plastic strain is calculated as

$$e_{pl} = e_{app} - \frac{S}{E_{app}} - e_1 . \qquad (1)$$

Here S is the nominal stress and e_{app} is the apparent nominal strain as measured by the apparatus. Further, E_{app} is the corresponding apparent modulus of elasticity including elastic deformation of both sample and machine parts. The apparent modulus of elasticity is defined from a linear fit to the experimental data between 20 and 80 % of the maximum nominal stress. Finally e_1 is taken from the intercept of the fitted line with the abscissa where the stress is zero. Figure 2 below shows the different parameters in equation 1 for clarity.

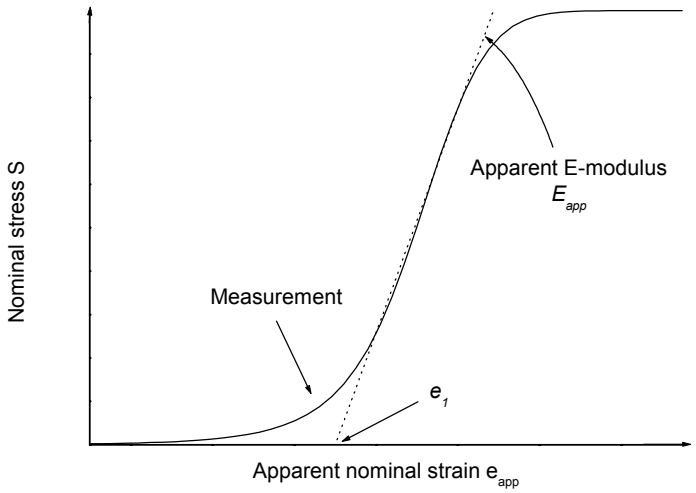

Figure 2. Schematic graph showing the different parameters used to extract the plastic strain in equation 1 from the original measurements.

It follows that the second term in equation 1, S/E_{app}, subtracts the elastic part of the deformation originating from both machine parts and sample, while e_1 subtracts possible play. It should be noted that in order to extract the plastic strain it is not necessary to know the true modulus of elasticity for the sample. Further, the true stress-strain curves are calculated until the onset of localised deformation and necking, assuming constant volume.

Apart from strain and temperature, the stress is also a function of strain rate. Mechanical testing with a commercial system, such as MTS, and using a constant cross head velocity thus leads to a decrease of the true strain rate since the specimen length is continually changed. The true strain rate can be calculated from

$$\dot{\varepsilon} = \frac{\dot{e}}{1+e} \qquad (2)$$

where $\dot{\varepsilon}$, $\dot{e}$ and e is the true strain rate, nominal strain rate and nominal strain respectively, see Dieter [5]. In the Hopkinson bar, the strain rate is a primary measured quantity and the strain is integrated from it. The changes of the strain rate are taken into account in the constitutive modelling discussed later.

With increasing strain rate the deformation process will gradually change from isothermal to adiabatic. For strain rates larger than about 1 s^{-1} there is no time for heat to dissipate and the deformation is mainly adiabatic. The adiabatic temperature increase can be calculated as

$$\Delta T = \frac{\varphi}{\rho C_p}\int_0^{\varepsilon}\sigma(\varepsilon)d\varepsilon\,. \qquad (3)$$

The temperature thus depends on the integrated deformation energy, the density ρ, and the heat capacity C_p. The parameter φ finally is a measure of the portion of the deformation energy which is converted into heat. This material constant is usually assumed to vary between 85 and 95 %, according to Meyer [6], but it has been shown by for example Macdougall and Harding [7] that this parameter may vary with the deformation. In this work,

it is assumed that 90 % of the deformation work is converted into heat. Further, both the density and the specific heat capacity vary with temperature. However, changes of the density are neglected and the figure given by the supplier at room temperature in table I is used as a constant. The specific heat capacity is measured as a function of temperature using a differential scanning calorimeter.

EXPERIMENTAL RESULTS

At quasi-static conditions the specimens show a linear elastic behaviour up to about 1300 MPa followed by a more or less constant nominal flow stress to fracture at a nominal strain of 5-10 %. The experimental scatter between the 12 different specimens is rather large and in the left part of figure 3 the curves with the lowest and highest measured flow stress are shown. The curves shown are not corrected according to equation 1. However, the value of E_{app} is of the order of 30-50 GPa, while Magness [1] gives a modulus of elasticity of about 340 GPa for a WHA alloy with a similar tungsten content of 93 %. As an example, the apparent modulus of elasticity is 47 GPa for the upper curve in figure 3 and e_1 equals 0.0045. These figures result in a plastic deformation of 0.064 at the onset of localised deformation which occurs at a total measured strain of 0.089 and a stress of 1400 MPa as obtained from figure 3.

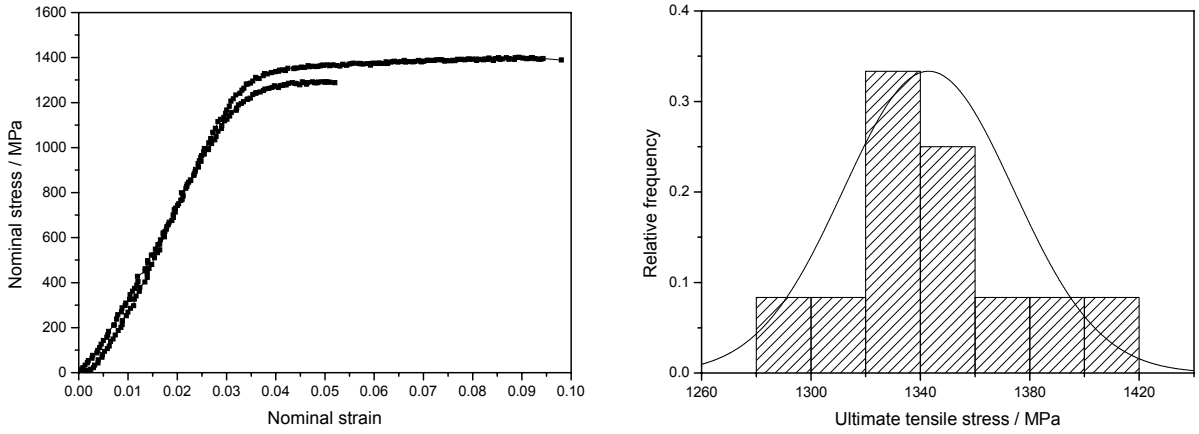

Figure 3. The left graph shows the quasi-static stress-strain curves for the samples with the highest and lowest measured nominal flow stress. The right part shows the relative frequency of the ultimate tensile stress for the 12 samples together with a corresponding Gauss curve.

The ultimate tensile stress for the 12 specimens varies between 1292 and 1400 MPa with an average and standard deviation of 1343 ± 31 MPa. In the right part of figure 3 the data are presented as a histogram together with a Gauss curve with the same average and standard deviation. According to the supplier the ultimate stress is 1350 MPa. The experimental scatter is rather large, and can be caused by inherent sample properties such as voids. However, effects of specimen preparation and uncertainties of the sample dimensions can not be excluded.

In figure 4 the effect of increasing strain rate and temperature on the flow behaviour of the tungsten heavy metal alloy can be seen. The experimental data are corrected according to equation 1 and the plastic true stress-strain curves are calculated assuming constant volume

during the deformation process. Data points collected after the onset of localised deformation are neglected and not shown.

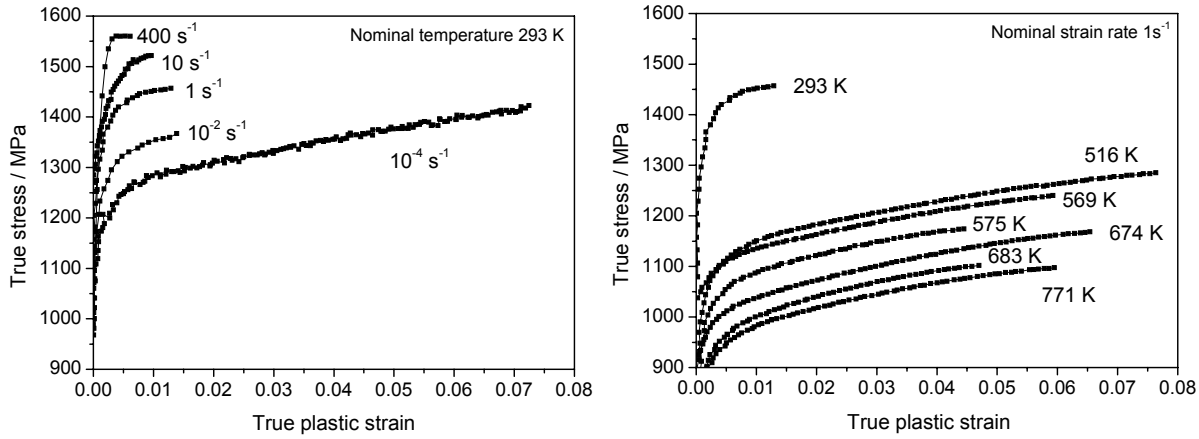

Figure 4. Stress-strain curves taken at a temperature of 293 K with different strain rates (left), and at a strain rate of 1 s^{-1} and varying temperatures (right). The figures indicate nominal strain rates and temperatures.

Obviously, the flow stress increases with increasing strain rate and decreases with increasing temperature. We also note that the strain to necking is small in the higher-strain-rate experiments carried out at room temperature, while the high temperature experiments give a larger strain even at a strain rate of 1 s^{-1}. The strain rates given in the left figure are nominal, and the constant cross head velocity used with the MTS-equipment gives a decrease of the true strain rate, as given by equation 2. For comparison, it is noted that at a true strain of 10 % the true strain rate is 10 % lower than the nominal strain rate. For the experiment with the Hopkinson bar giving the highest nominal strain rate of 400 s^{-1}, the points in the graph correspond to true strain rates between about 350 s^{-1} and 600 s^{-1}.

With increasing strain rate the deformation process will gradually change from isothermal to adiabatic and, as pointed out above, for strain rates larger than about 1 s^{-1} the deformation is mainly adiabatic. The temperature increase can be calculated from equation 3 and depends on the deformation energy, the density ρ, and the heat capacity C_p. Density changes with temperature are neglected and the value of 17700 kg/m^3 is used as a constant, see table I. The specific heat capacity, on the other hand, is measured as a function of temperature using a differential scanning calorimeter and shown in figure 5.

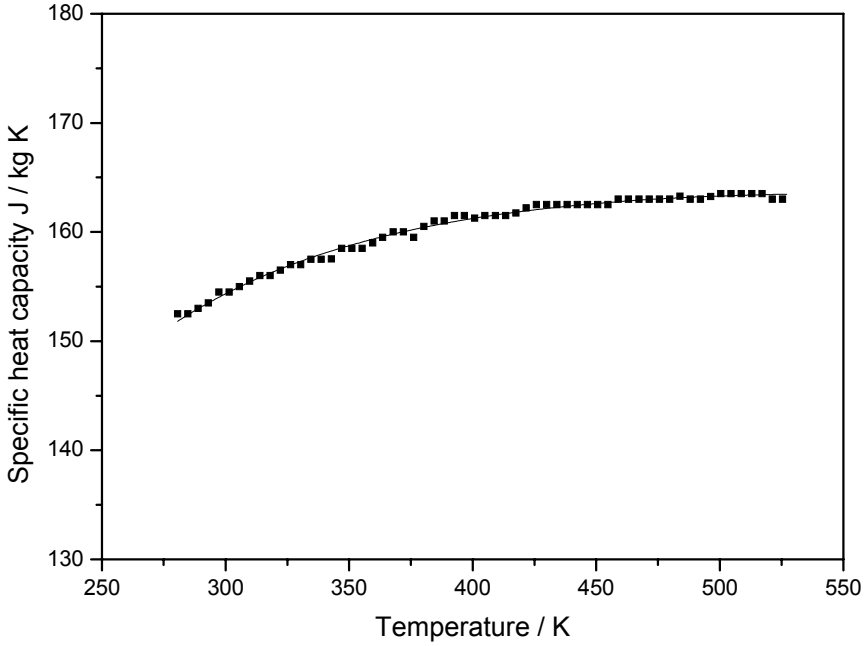

Figure 5. Specific heat capacity as a function of temperature, measured with a differential scanning calorimeter at a heating rate of 10 K/min. The data points are averages of two different measurements with an individual scatter of less than 2.5 %. The curve is a fit to the averaged data with parameters according to equation 4.

As seen, at room temperature the specific heat capacity is close to 150 J/kgK, while pure tungsten has 133 J/kgK [8] and another tungsten heavy metal alloy is assigned a figure of 134 J/kgK [9]. It is also noted that the temperature dependency of the heat capacity is rather low, with an increase from room temperature of only about 10 J/kgK to about 160 J/kgK at a temperature of 500 K. The data above suggest a maximum solid heat capacity close to 165 J/kgK. A function has been fitted to the results, giving the relation

$$C_p(T) = 181.3 - 0.02121 \cdot T - 1856 \cdot 10^3 \cdot T^{-2} \qquad (4)$$

which is later incorporated in the calculation of the adiabatic flow stress curves. It is emphasised that the equation only is intended for interpolation and should not be used to extrapolate the specific heat capacity to temperatures outside the experimental range. From equations 3 and 4 together with results presented in figure 4 the temperature increase during the adiabatic deformation modes, i.e. strain rates from 1 s^{-1} and higher is determined. It is found that due to the small deformations before failure all high strain rate experiments at room temperature result in a very small temperature increase of less than 5 °C. The data collected at enhanced temperatures and a strain rate of 1 s^{-1} seen in the right part of figure 4 give a maximum temperature increase of the order of 30 °C. Although rather small, the temperature change is incorporated in the model fitting discussed below.

In an effort to give a mathematical description of the material behaviour, the constitutive equations developed by Johnson and Cook [3] as well as the one proposed by Zerilli and Armstrong [2] have been fitted to the experimental results.

CONSTITUTIVE MODELLING

Accurate descriptions of the response of materials over a wide range of loading conditions as well as predictive capabilities outside the experimentally available range are in great demand. Thus, a number of different models have been developed to describe the response of metals to mechanical deformation, see for example Meyer [6]. The constitutive equations presented by Johnson and Cook [3] (J&C) in 1983 and the one suggested by Zerilli and Armstrong [2] (Z&A) in 1986 are both implemented in finite element codes, such as LS-DYNA and AUTODYN. As a consequence, these models are often used for calculations involving large deformations and high strain rates and they are briefly described below. In both models, the flow stress is a function of strain, strain rate and temperature. In the fitting procedure all data shown in figure 4 are used and changes in true strain rate and temperature during the deformation process is taken into account. It follows that each stress value is assigned to a unique strain, strain rate and temperature and exactly the same set of data are used to extract both the J&C and the Z&A model constants. Further, the constitutive parameters are determined simultaneously by using a non-linear fitting procedure supplied by the Origin software version 6.1 [10].

The Johnson and Cook model

In 1983 Johnson and Cook [3] presented the semi-empiric constitutive model

$$\sigma = \left(\sigma_0 + A\varepsilon^n\right)\left(1 + B\ln\frac{\dot{\varepsilon}}{\dot{\varepsilon}_0}\right)\left(1 - \left(\frac{T - T_r}{T_m - T_r}\right)^m\right) \qquad (5)$$

to describe the relation between flow stress σ (Pa), strain ε, strain rate $\dot{\varepsilon}$ (s^{-1}) and temperature T (K). In this equation, T_r and $\dot{\varepsilon}_0$ are a reference temperature (usually room temperature) and reference strain rate (usually 1 s^{-1}), respectively, at which the material parameters σ_0 (Pa), A (Pa) and n are determined. The constant B in the second term takes the strain rate dependency into account. Finally, in the third term, T_m is the melting temperature and m is a parameter that represents the effect of temperature on the flow stress. It is emphasised that the model is semi-empirical and that influence of strain (the first factor), strain rate (the second factor) and temperature (the third factor) are decoupled from each other. If the deformation occurs isothermally with $T = T_r$, the third factor in equation 5 equals unity.

By use of the experimental data in figure 4, the Johnson and Cook material parameters are simultaneously deduced by a non-linear fit of the model parameters to the experiments. In table II the resulting material parameters are shown, together with the standard errors. In the table, J&C parameters found in the literature [3, 11] for similar tungsten heavy metal alloys with a matrix of nickel and iron are also given. The WHA investigated in this report contains 92.5 % tungsten, but cobolt is added to the matrix. The work by Weerasooriya [11] is based on torsional strain rates of 10^{-4}, 10^{-1} and 600 s^{-1} conducted at room temperature. At a strain rate of 10^{-2} s^{-1}, experiments were also carried out at 197 K and 408 K. The model parameters given by Weerasooriya [11] are for shear stress with a reference shear strain rate of 0.1 s^{-1}. Further, the temperature dependency of the flow stress in the original J&C-model (see equation 5) is written as $(1-((T-T_r)/(T_m-T_r))^m)$, while Weerasooriya used $(1-(T-T_r)/(T_m-T_r))^m$. It is finally noted that Weerasooriya appears to have used the melting point of tungsten (T_m =

3683 K) instead of that of the matrix ($T_m \approx 1723$ K) when extracting model parameters. The parameters presented by Johnson and Cook are valid for equivalent axial stress but deduced from torsional experiments at a maximum shear strain rate of about 400 s^{-1}. Further, the experiments were carried out at room temperature and the thermal softening parameter was assumed to be one (m = 1). The torsional equipment used by the authors mentioned allows a larger deformation before fracture compared to tensile testing and if the von Mises flow rule is applied an equivalent tensile flow stress can be calculated.

Table II. Johnson and Cook material parameters for some tungsten heavy metal alloys.

Parameter	This work[a]	Johnson and Cook [3] [b]	Weerasooriya [11] [c]
σ_0 / MPa	631 ± 114	1506	729
A / MPa	1258 ± 97	177	139
n	0.092 ± 0.014	0.12	0.413
B	0.0140 ± 0.0003	0.016	0.0366
m	0.940 ± 0.007	1	4
ρ / g cm^{-3}	17.7	17.0	17.7
Content / w%	92.5% W, (Ni, Fe, Co)	90% W, (Ni, Fe)	93% W, (Ni, Fe)

[a] *Parameters for J&C equation 5.*
[b] *Parameters for J&C equation 5, extracted from torsional data. The constant m is assumed to be 1.*
[c] *Parameters for torsional data with reference shear strain rate of 0.1 s^{-1} and modified temperature dependency.*

In figure 6 the agreement between the model deduced in this work and the experimental results is shown. The calculated flow stress curves are found by using the experimental values of true strain, true strain rate and temperature in connection with equation 5 and the model parameters in table II. For clarity some of the curves have been omitted in figure 6. Following Johnson and Cook, the melting temperature of the WHA alloy used in the J&C equation was set to 1723 K which is close to the melting point of the metal matrix.

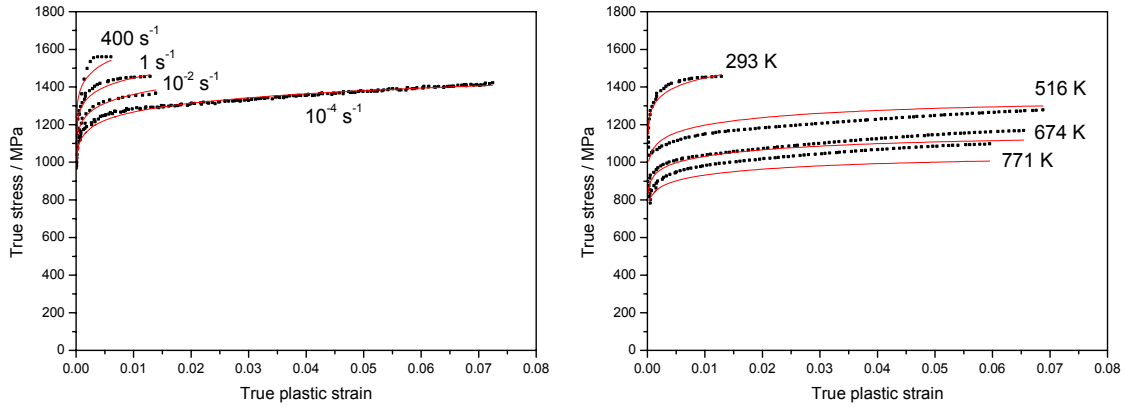

Figure 6. Comparison between the J&C model and experimental data at 293 K for varying strain rates (left) and at a strain rate of 1 s^{-1} but different temperatures (right). The deviation between calculation and experiment is of the order of 5-10 %. Indicated temperatures and strain rates are nominal values.

The best fit was chosen so that the sum of the squares of the deviations between the theoretical curves from the experimental points is minimised. The fitting above corresponds to a coefficient of determination (or R^2 value) of 0.94, while a value of unity would indicate that the sum of the squared deviations is zero. It is also seen that the model can reasonably reproduce the experimental strain rate dependency in the left figure, while the deviation is higher at elevated temperatures as seen in the right graph.

Considering the literature data, Weerasooriya reported a deformation hardening at the lowest shear strain rates (10^{-4}, 10^{-1} s^{-1}). In contrast, the flow stress decreases with increasing strain at the highest deformation rate of 600 s^{-1}, interpreted as an effect of thermal softening. The parameters presented by Johnson and Cook also give thermal softening of the flow stress at very low strains at adiabatic deformation modes, see also figure 7.

From comparison of the data found in this work with the other parameter set for equation 5, given by Johnson and Cook, it is noted that the parameters σ_0 and A in the first factor of the constitutive relation differ significantly. This leads to significant differences in flow stress at very small deformations. However, at strains larger than about 5 % the combination of the parameters lead to a more similar deformation behaviour. Turning to the other constants, representing deformation rate (B) and thermal effects (m) it is found that the differences are much smaller. In general, for conventional WHA alloys containing 90-93 % tungsten with a nickel-iron matrix the strain rate hardening and thermal softening are almost the same as discussed by Yadav et al. [12].

In figure 7, a comparison between the model curves calculated using data presented by Johnson and Cook and the parameters deduced in this work can be made. In this figure the adiabatic flow stress curves are shown, because at large strains and high strain rates the effect of adiabatic heating can not be neglected and the temperature increase has to be calculated and incorporated in the constitutive equations. This is done by using equation 3 together with a temperature-dependent specific heat capacity as seen in equation 4. Thus, from the yield stress a new flow stress was calculated from a small increase in strain using the J&C (or the Z&A, see also figure 10) constitutive relation and a start value of the temperature. From this new stress-strain pair a new temperature is deduced from equation 3 using the previous heat capacity value. Finally, a new heat capacity was calculated from relation 4 and thus the values of all necessary parameters have been renewed and the next calculation loop can begin, starting with a new small increase of the strain. In the calculations shown in figure 7 below the small step increase in strain was set to 0.001 giving temperature changes of fractions of a degree for each calculation loop and thus avoiding significant errors due to the step increase of the strain.

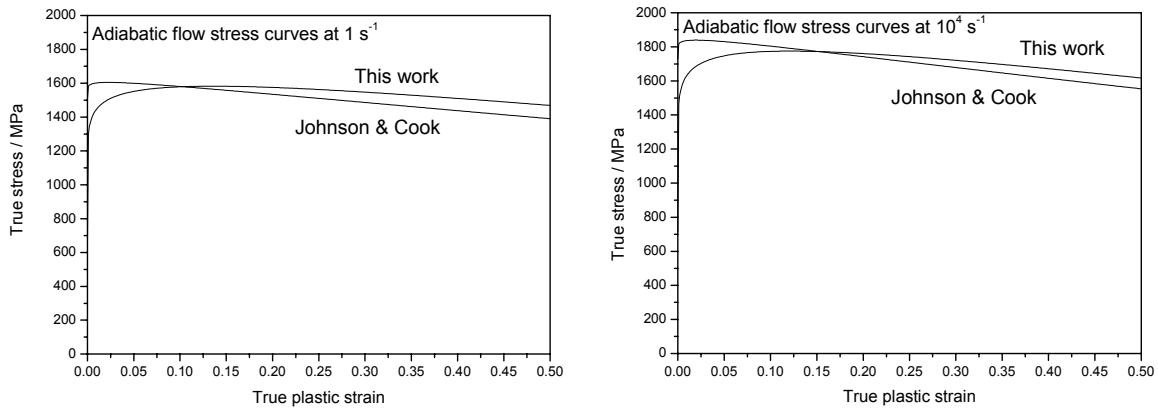

Figure 7. Comparison of the predicted flow stresses using the different Johnson and Cook material models given by column 2 and 3 in table II. The nominal temperature is 293 K.

From figure 7 it is clear that after an initial deformation of about 5 %, the curves show a more similar behaviour differing in the absolute value of the flow stress with about 50-150 MPa or

roughly 10 %. It is also found that at a strain of 50 % and a strain rate of 10^4 s^{-1} the temperature is about 560 K for both model sets.

For the errors associated with the parameters given in table II, no thorough sensitivity analysis of the effect on the resulting flow stress was made. However, changing one of the parameters to the estimated minimum value within the given error interval keeping the other at their nominal values results in a change of the flow stress of up to a maximum of 80 MPa at a strain rate of 10^4 s^{-1} and a strain of 50 %. The largest change emerges from σ_0, i.e the flow stress at the reference strain rate and reference temperature at zero plastic strain.

The Zerilli and Armstrong model

The constitutive relation developed by Zerilli and Armstrong [2] has the general form

$$\sigma = C_1 \varepsilon^m e^{(-C_2 T + C_3 T \ln \dot{\varepsilon})} + C_4 + C_5 \varepsilon^n + k d^{-1/2}. \qquad (6)$$

This model is modified depending on the crystal structure of the material investigated and has also been extended to allow for other effects such as twinning [13]. Here C_1 to C_5, n, m and k are inherent material parameters, while d is the grain size and the other quantities are the same as in the J&C model. The thermally activated part of the flow stress is described by the first term, while the athermal part is given by C_4 and the effect of grain size is given by the Hall-Petch relation ($kd^{-1/2}$). For face centred cubic (FCC) crystal structures the deformation hardening is dominated by forest dislocation interactions and the stress is proportional to the square root of plastic strain, with m equal to 0.5 and C_5 = 0. For body centred cubic (BCC) crystal structures, (such as tungsten) the inherent Peierls lattice stress is predominant and the parameter m equals zero. Further, for a constant grain size the term $kd^{-1/2}$ can be incorporated in the athermal component C_4 of the flow stress and the Z&A equation can be written as

$$\sigma = C_1 e^{(-C_2 T + C_3 T \ln \dot{\varepsilon})} + C_4 + C_5 \varepsilon^n. \qquad (7)$$

Thus, if the contribution from the matrix to the deformation is neglected, the deformation for the heavy metal alloy can be described with the Z&A constitutive model for BCC-structures. It must be pointed out that the parameter C_4 in equation 7 is independent of strain, strain rate and temperature and thus should be treated as a constant in the fitting procedure. Further, Lee and Chiou [14] who investigated the deformation of a WHA composite report that at low strain rates ($4 \cdot 10^{-3}$ s^{-1}) the main deformation was concentrated in the matrix. At higher stresses and strain rates, obtained with a torsional split Hopkinson system, the deformation of the tungsten grains dominate. Work by Wittman and Lopatin [15] also shows that the deformation is governed by the tungsten grains at high strain rates. This is also discussed by Lennon and Ramesh [16] in a work on the thermomechanical response of pure tungsten in compression. It is also noted that the deformation of WHA is reported to occur mainly in the matrix at small strains, while the deformation of the tungsten grains increases with increasing plastic work as discussed by Magness [1]. These strain- and strain rate dependent deformation modes further complicate the development of a constitutive model for tungsten heavy metal alloys applicable to a large range of strains and strain rates. In this report the overall deformation is assumed to be dominated by the BCC tungsten grains, and equation 7 is used to model the

plastic flow stress. Moreover, it is known that some alloy steels and materials with a hexagonal closed packed (HCP) structure such as high purity titanium show both FCC and BCC characteristic behaviour. For these cases a model that incorporates both effects has been developed by Zerilli and Armstrong [13, 17]. Even so Macdougall and Harding [18] uses a BCC formulation of the Z&A constitutive equation to describe a titanium alloy (Ti-6Al-4V) with a hexagonal closed packed (HCP) structure.

Finally, there is also some evidence that a temperature dependency exists for parameters that are outside the temperature dependent part in equations 6 and 7. This is discussed by, among others, Goldthorpe et al. [19].

For the Zerilli and Armstrong constitutive equation, the parameters are found by a non linear fit of the same set of data (see figure 4) as in the fitting of the Johnson and Cook parameters. Thus, the experimental stress is related to a true strain, true strain rate and a temperature incorporating adiabatic heating for the higher strain rates, as discussed earlier. In table III the resulting material constants can be studied together with the error estimates. Only one other data set for Z&A model parameters has been found in the literature for WHA alloys. Lee, Xiea and Lin [20] investigated a WHA with 92.5 % W, 5.25 % Ni and 2.25 % Fe using a compression split Hopkinson apparatus at strain rates from $8 \cdot 10^2$ to $4 \cdot 10^3$ s^{-1} and temperatures between 25 and 1100 °C. They also used the BCC form of the Z&A equation when interpreting their data. Unfortunately, as seen in table III, one of the derived material constants (C_3) is missing in their paper. However, model constants for pure tungsten collected by Bourne et. al. [21] and for extruded tungsten determined by Lennon and Ramesh [16] are also presented in table III for comparison.

Since the available data set in this work does not include any information about grain size, the parameter C_4 is only used as a constant in the fitting procedure. The value of 100 MPa corresponds to a grain size of about 50 μm using the equation presented by Bourne and given in table III. It is also noted that using other "reasonable" values of the constant C_4 (between 0 and 400 MPa) the resulting Zerilli and Armstrong equations are almost equivalent. The calculated flow stresses deviates less than 10 MPa for the range of strain, strain rate and temperature given in figure 8 below. Extrapolating the equations to a strain rate of 10^4 s^{-1} and a strain of 50 % the deviation in flow stress between the different Z&A parameter sets increases slightly to about 40 MPa. In the work by Lee et al. [20] they assumed $C_4 = 0$ in their fitting approach to the Z&A model. As a comparison, if the parameter C_4 is set to 0 in the present data set the fitting procedure results in $C_1 = 1379$ MPa, $C_2 = 0.0025$ K^{-1}, $C_3 = 0.00011$ K^{-1}, $C_4 = 0$ MPa, $C_5 = 1129$ MPa and $n = 0.081$. As seen, only the parameters C_5 and n affecting the strain hardening changes, with a small increase in C_5 and a slight decrease of n compared to the result presented in table III. The net result of these changes is indeed very small and the calculated flow stresses deviate less than 1 % in the experimental range of strain, strain rate and temperature.

Table III. Z&A model parameters.

Parameter	WHA (This work)	WHA (Ref [20])	Extruded tungsten (Ref [16])	Pure tungsten[a] (Ref [21])		
C_1 / MPa	1381±14	1287	2749.0	16500	24900	41000
C_2 / K^{-1}	0.0025±0.0001	0.00019	$2.2552 \cdot 10^{-3}$	0.591	0.666	0.061
C_3 / K^{-1}	$0.00011 \pm 4 \cdot 10^{-6}$	Missing	$9.0541 \cdot 10^{-3}$	0.000279	0.000307	0.000307
C_4 / MPa	100[b]	0[b]	49.908 [b]	$25.6 \cdot d^{-0.5}$	$25.6 \cdot d^{-0.5}+20$	$25.6 \cdot d^{-0.5}+20$
C_5 / MPa	1047±16	826	194.49	860	860	860
n	0.093±0.003	0.287	0.050513	0.443	0.443	0.443

[a] *Material data collected by Bourne et al. [21], where d is the grain size (in mm) of the tungsten particles.*
[b] *Used as a constant in the fitting procedure, see text above.*

In figure 8 the calculated and experimental flow stress curves are compared for some cases. With use of the experimental values of true strain, true strain rate and temperature (including deformation induced heating) and the extracted material parameters the calculated stress is found from equation 7 and compared with the experimental stress. It is seen that the agreement between experiment and model is rather good with a deviation of less than about 5 %. The largest deviation is found at the highest strain rate of 400 s^{-1}. The fitting result corresponds to a coefficient of determination (or R^2 value) of 0.97. In general, the fit between model and experiment is better for the Zerilli and Armstrong model than for the Johnson and Cook model, see figure 6, which results in a R^2 value of 0.94.

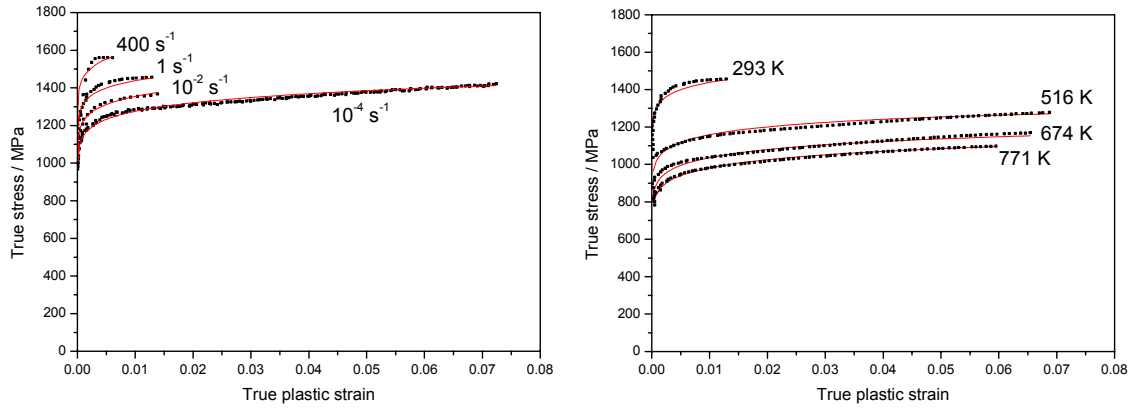

Figure 8. Comparison between the Z&A model and experimental data at 293 K for varying strain rates (left) and at a strain rate of 1 s^{-1} but different temperatures (right). The deviation between calculated flow stress and experiment is less than 5 %. Indicated temperatures and strain rates are nominal values.

As in the case with the Johnson and Cook model parameters, no comprehensive sensitivity analysis of the effect of the uncertainty of the Z&A model constants to the resulting flow stress curve was done. Moreover, the parameters in the Zerilli and Armstrong equation are coupled which makes it difficult to extract the effect of the different constants on the stress. Nevertheless, it is noted that if the parameters are changed to the lower error limit keeping the other constants at their nominal values the flow stress is changed less than 30 MPa at a strain of 50 % and a strain rate of 10^4 s^{-1}.

Model comparisons

As discussed, the Zerilli and Armstrong model gives a better agreement between model and experiment than the constitutive equation developed by Johnson and Cook. The same set of data are used in both model fittings and comparing model with experiment the J&C and Z&A equations result in R^2 values of 0.94 and 0.97 respectively, see also figures 6 and 8. At high strain rates and also at high temperatures the J&C model deviates significantly from experiment. The constitutive equation by Z&A, on the other hand, reflects the experimental values more or less equally well independently of strain rate and temperature.

It should also be noted that both the J&C and the Z&A models use a power law for the flow stress with a continual strain hardening without saturation for the flow stress at large strains. These constitutive models also assume that the strain hardening is independent of strain rate and temperature. This has been discussed by several authors [18, 22] and some attempts to introduce a temperature correction of the deformation hardening parameters have been made. Chen and Gray [22] show that the hardening behaviour in a constitutive model that uses a power hardening law depends on the strain range within which the coefficients are optimised, and suggests that a saturation stress should be used at large strains. It is also known that the hardening behaviour may also be a function of the strain rate, see Chen and Gray [22]. In the present investigation most of the data are collected at a strain rate close to $1s^{-1}$, as seen in figure 4, and this will obviously affect the value of the fitting parameters. Moreover, in this specific investigation of WHA the low tensile strains achieved before fracture makes it difficult to draw any decisive conclusions on the strain hardening behaviour.

As discussed, the material models are frequently used for extrapolation of the flow stress to very high strains, strain rates and deformation induced temperatures and in figure 9 the calculated flow stresses are shown for strain rates of 10^{-4}, 1 and 10^4 s^{-1} for both the J&C and the Z&A equations.

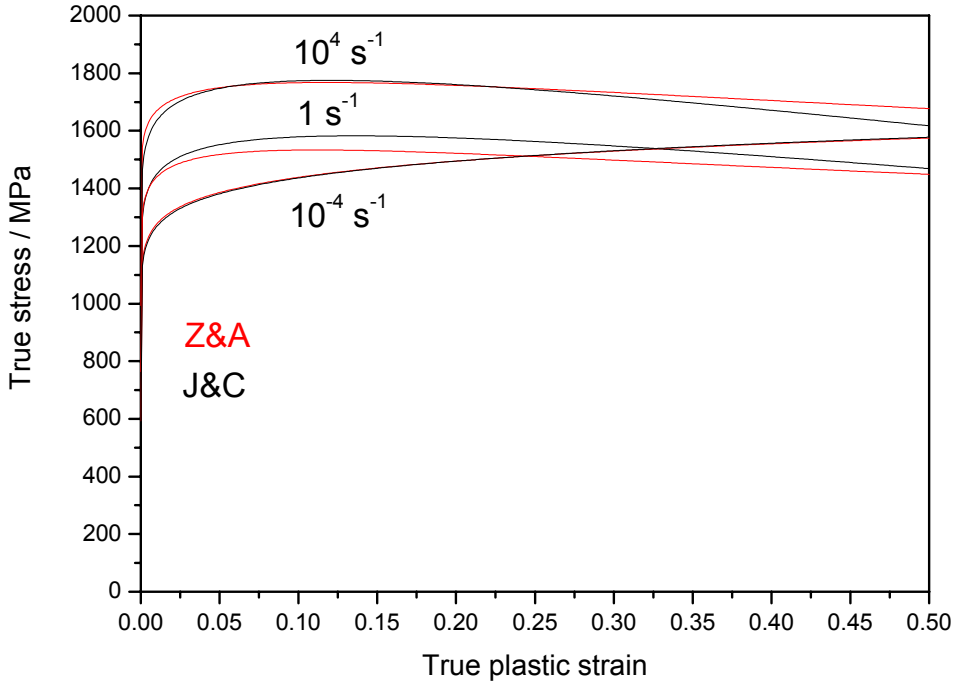

Figure 9. Calculated flow stress curves using the Z&A (red) and the J&C (black) constitutive equations for the adiabatic strain rates of 1 and 10^4 s^{-1} and the isothermal strain rate of 10^{-4} s^{-1}.

From figure 9 it is obvious that the flow stress reaches a maximum at a strain of approximately 10-15 % for the high adiabatic strain rates due to the effect of thermal softening. The low, isothermal, strain rate on the other hand gives a continuing hardening without any maximum. For the adiabatic cases at 10^4 s^{-1} the temperature increases almost linearly with strain to a value of about 560 K at a strain of 50 %, independent of model. Moreover, it is found that the largest discrepancy between the J&C and the Z&A constitutives is found in the intermediate strain rate of 1 s^{-1}, where the difference is approximately 100 MPa for most of the range shown.

As discussed, these equations are frequently used for extrapolation of the flow stress to very high strains, strain rates and deformation induced temperatures. According to Zerilli and Armstrong [2], the range of applicability of the model is for temperatures up to about half of the absolute melting temperature. The upper strain rate is limited by the maximum dislocation velocity which is near the elastic shear wave speed. At extremely high strain rates the models are not applicable, since the deformation is governed by dislocation generation. For low strain rates on the contrary, diffusion and dynamic recovery must be analysed. The Johnson and Cook equation is more empirical but it is likely that the range of application is similar and it is known [6] that the flow stress increases faster than predicted at strain rates higher than about 10^3 s^{-1}. Finally, it is emphasised that both models are mainly intended for rather large plastic deformations and cannot be used to describe effects at small strains.

CONCLUDING REMARKS

At quasi-static conditions the investigated tungsten heavy metal alloy shows elastic behaviour up to a stress of about 1300 MPa followed by plastic deformation with rather low strain hardening. It is found that the ultimate tensile stress at quasi-static conditions for the 12 investigated samples is 1340 MPa with a standard deviation of 30 MPa. The average is in good agreement with the figure of 1350 MPa given by the supplier. The maximum measured difference in ultimate tensile stress is about 100 MPa, and fracture occurs at a nominal strain of the order of 5-10 %.

At increasing strain rate, the ductility shows a marked decrease and for tensile strain rates from 0.01 s^{-1} and higher, elongation to failure is only of the order of 1 %. The flow stress on the other hand increases with strain rate and is about 1550 MPa at the highest investigated nominal strain rate of 400 s^{-1}. Experiments conducted at a strain rate of 1 s^{-1} but at a temperature close to 200 °C give a decrease in flow stress of about 250 MPa compared to room temperature, while the strain at fracture goes from 1 % to about 8 %.

Considering the constitutive modelling, a BCC form of the Zerilli and Armstrong equation has been used, although the WHA material is a composite of a metal matrix with FCC-structure embedding tungsten grains with BCC-structure. At high strain rates and large deformations the main deformation occurs in the BCC tungsten grains, while the matrix is more deformed at low strain rates or small strains. This strain and strain rate dependent change of deformation mode further complicates the development of a constitutive equation for WHA alloys. A model that incorporates properties for both the matrix and the tungsten grain should be an improvement.

Despite the above discussion it is also noted that the Z&A model show a good agreement with experimental data, while the deviation between the J&C parameters and measured data is

higher. It is again pointed out that flow stress data at larger strains are urgently needed to improve the model fitting. For the purpose of hydrocode penetration calculations, another equally important area is the development of reliable fracture and damage models and determination of the associated material parameters.

ACKNOWLEDGEMENTS

The author is grateful to Juhani Vassfjord for the mechanical experiments and the development of a reliable testing procedure at enhanced temperatures. Ass. Prof. Fransson at the university of Umeå is acknowledged for the measurement of the specific heat capacity on the tungsten heavy metal alloy investigated. Finally, the comments on the manuscript from various colleagues at FOI are appreciated.

REFERENCES

[1] L. S. Magness, "A phenomenological Investigation of the Behavior of High-Density Materials Under the High Pressure, High Strain Rate Loading Environment of Ballistic Impact", Dissertation, John Hopkins University, Baltimore, Maryland 1992.

[2] F. J. Zerilli and R. W. Armstrong, "Dislocation-mechanics based constitutive relations for materials dynamics calculations", *Journal of Applied Physics*, vol. 61, p. 1816, 1986.

[3] G. R. Johnson and W. H. Cook, "A constitutive model and data for metals subjected to large strains, high strain rates and high temperatures", presented at 7th Int. Symp. on Ballistics, Hauge, Netherlands, 1983.

[4] T. Svensson, "A pendulum impactor for confident tensile testing at high rates of strain", National defence research institute, Stockholm, FOA report C 20577-D4, June 1985.

[5] G. E. Dieter, *Mechanical Metallurgy*: McGraw-Hill, 1988.

[6] M. A. Meyers, *Dynamic Behavior of Materials*: John Wiley & Sons, Inc., 1994.

[7] D. A. S. Macdougall and J. Harding, "The measurement of specimen surface temperature in high-speed tension and torsion tests", *International Journal of Impact Engineering*, vol. 21, p. 473, 1998.

[8] C. Nordling and J. Österman, "Physics Handbook", Lund: Studentlitteratur, 1987.

[9] AUTODYN, "Theory manual", Century Dynamics Ltd., Horsham, UK, 1995.

[10] Origin, *Origin User's Manual, Data Analysis and Technical Graphics Software*, Northamton, MA 01060, USA: Microcal Software Inc., 1999.

[11] T. Weerasooriya, "Modeling flow behavior of 93%W-5Ni-2Fe tungsten heavy alloy", presented at High-Pressure Science and Technology, Colorado springs, Colorado, USA, 1993.

[12] S. Yadav, E. A. Repetto, G. Ravichandran and M. Ortiz, "A computational study of the influence of thermal softening on ballistic penetration in metals", *International Journal of Impact Engineering*, vol. 25, p. 787, 2001.

[13] F. J. Zerilli and R. W. Armstrong, "Dislocation Mechanics Based analysis of Material Dynamics Behaviour: Enhanced Ductility, Deformation Twinning, Schock Deformation, Shear Instability, Dynamic Recovery", *Journal de Physique IV, Colloque C3*, vol. 7, p. 637, 1997.

[14] W.-S. Lee and S.-T. Chiou, "The influence of loading rate on shear deformation behaviour of tungsten composite", *Composites*, vol. 27B, p. 193, 1996.

[15] C. L. Wittman and C. M. Lopatin, “Determination and application of constitutive material model constants for a tungsten two phase alloy” presented at International conference on tungsten and tungsten alloys, Arlington, Virginia, USA, 1992.

[16] A. M. Lennon and K. T. Ramesh, “The thermoviscoplastic response of polycrystalline tungsten in compression”, *Materials Science and Engineering A*, vol. A276, p. 9, 2000.

[17] F. J. Zerilli and R. W. Armstrong, “Constitutive relations for titanium and Ti-6Al-4V” in *Shock compression of condensed matter*, Schmidt (ed.), 1995.

[18] D. Macdougall and J. Harding, “Materials testing for constitutive relations”, *Journal de Physique IV, Colloque C3*, vol. 7, p. 103, 1997.

[19] B. D. Goldthorpe, “Constitutive equations for annealed and explosively shocked iron for application to high strain rates and large strains”, *Journal de Physique IV, Colloque C3*, vol. 1, p. 829, 1991.

[20] W.-S. Lee, G.-L. Xiea and C.-F. Lin, “The strain rate and temperature dependency of the dynamic impact response of tungsten composite”, *Materials Science and Engineering A*, vol. 257, p. 256, 1998.

[21] B. Bourne, K. G. Cowan and J. P. Curtis, “Shaped Charge Warheads Containing Low Melt Energy Metal Liners” presented at 19:th International Symposium of Ballistics, Interlaken, Switzerland, 2001.

[22] S. R. Chen and G. T. Gray III, “Constitutive behaviour of tantalum and tantalum-tungsten alloys”, *Metallurgical and materials transactions A*, vol. 27A, p. 2994, 1996.